Supporting Information

Banchereau et al. 10.1073/pnas.1205785109

SI Materials and Methods

DC Subsets. $CD34^+$-derived DCs were generated in vitro from $CD34^+$ HPCs isolated from the blood of healthy volunteers given GM-CSF (Neupogen) to mobilize precursor cells. HPCs were cultured at 0.5×10^6 cells per mL in Yssel's medium (Irvine Scientific) supplemented with 5% (vol/vol) autologous serum, 50 μM β-mercaptoethanol, 2 mM L-glutamine, 1% (vol\vol) penicillin/streptomycin, GM-CSF (50 ng/mL; Leukine), Flt3-L (100 ng/mL; R&D), and TNF-α (10 ng/mL; R&D) for 9 d. Media and cytokines were refreshed at day 5 of culture. Subsets of DCs, $CD1a^+CD14^-$ LCs, and $CD1a^-CD14^+$ DCs were then sorted, yielding a purity of 95–99%. Epidermal LCs (skin LCs) and dermal $CD14^+$ DCs were purified from normal human skin specimens. Specimens were incubated in bacterial protease dispase type 2 for 18 h at 4 °C and then for 2 h at 37 °C. Epidermal and dermal sheets were then separated, cut into small pieces (~1–10 mm), and placed in RPMI 1640 supplemented with 10% FBS. After 2 d, the cells that migrated into the medium were collected and further enriched by using a Ficoll-diatrizoate at a density of 1.077 g/dL DCs were purified by cell sorting after staining with anti-CD1a FITC (DAKO) and anti-CD14 APC mAbs (Invitrogen).

DC/T-Cell Cocultures. For autologous primary response assessments, naïve $CD8^+$ T cells ($CD8^+CCR7^+CD45RA^+$; 1×10^6 cells per well) were stimulated with in vitro-generated LCs or $CD14^+$ DCs (5×10^4 cells per well) that were preincubated for 3 h with the HLA-A201–restricted MART-1 (26-35, ELAGIGILTV), gp100 (209-217, IMDQVPFSV), or a control peptide (3 μM) in the presence of anti-CD8 (RPA-T8, BD Biosciences; T8, Beckman Coulter; or OKT8) or isotype control antibody (at indicated concentration). Cells were cultured for 9 d with IL-7 (10 U/mL; R&D) and CD40L (100 ng/mL; R&D). IL-2 (10 U/mL; R&D) was added at day 3. Expansion of peptide-specific $CD8^+$ T cells was determined by counting the number of cells binding peptide/HLA-A201 tetramers (Beckman Coulter) at the end of the culture period, as well as the CD8 mean florescence intensity on the tetramer binding cells. For the assessment of secondary response, autologous purified $CD8^+$ T cells or sorted memory $CD8^+$ T cells (1×10^5 cells per well) were cultured with LCs or $CD14^+$ DCs (5×10^3 cells per well), preloaded with 1 μM HLA-A201–restricted Flu-MP–peptide (58-66, GILGFVFTL), and cultured with in the presence of anti-CD8 or isotype control antibody (3 μg/mL unless otherwise indicated). Cells were cultured for 9 d in Yssel's complete medium supplemented with IL-7 (10 U/mL) and CD40L (100 ng/mL). IL-2 (10 U/mL) was added at day 3. Expansion of peptide-specific $CD8^+$ T cells was determined by counting the number of cells binding peptide/HLA-A201 tetramers (iTAg; Beckman Coulter) at the end of the culture period. iTAg tetramers possess a mutation that minimizes the aberrant effect that some CD8 antibodies might have on the specific binding of MHC class I tetramer (1). For primary allogeneic $CD8^+$ T-cell culture, sorted naïve T cells were cultured with allogeneic-sorted mDC subsets, generated in vitro from $CD34^+$ HPCs, or isolated from skin at a ratio of 1:40. Where indicated, anti-CD8 mAb, soluble ILT-Fc fusion proteins, or anti-ILT receptor Ab was added at the indicated concentration. Cell proliferation was assessed by the level of thymidine incorporation after 5 d or CFSE dilution (0.5 μM CFSE; Invitrogen). Expression of effector molecules granzyme A (BD Pharmingen), granzyme B (eBiosciences), and perforin (Fitzgerald) and surface molecules CD30, CD40L, and CD25 (all from BD Biosciences), were analyzed after 7 d by flow cytometry. For intracellular cytokine analysis, day 7-primed $CD8^+$ T cells were restimulated for 24–40 h with either fresh DC or a combination of immobilized anti-CD3 (BD Biosciences) and soluble anti-CD28 (2 μg/mL; eBiosciences) in fresh medium containing IL-2 (10 IU/mL). Intracellular IL-2, IFN-γ, TNF-α, IL-4, or -13 (all from BD Biosciences) expression was assessed by flow cytometry after additional 5-h stimulation with PMA (25 ng/mL; Sigma) and ionomycin (1 μM; Sigma). Cytokines in the culture supernatant of $CFSE^{lo}CD11c^-CD4^-$ $CD8^+$ T cells (1.5×10^5 cells per ml) were measured by Luminex after 48-h restimulation with anti-CD3 and -CD28 mAbs.

Cloning of ILT-Fc Molecules and Generation of ILT-Specific mAbs. Vectors for the expression in stably transfected CHO-S cells of ILT–IgFc proteins were hILT2 GI:12636295 226-1602, hILT3 GI:85567629 20-1349, hILT4 GI:2660709 3-1376 with G13C and A18G changes, or hILT5 GI:2665646 3-1332 residues preceded by acc inserted into CET1019HS-puro-SceI (Millipore) in the Fse I–Nhe I interval with either GI:308035026 520-1017 preceded by gctagc and followed by caccatcaccatcaccattgagcggccgc or GI:194381819 774-1470 preceded by gctagccaccggt and followed by gcggccgc in the Nhe I–BstB I interval. Procedures for transfection and cell culture were as described (2), and purification of IgFc fusion proteins was as described (3). Procedures for immunization of mice, derivation of hybridomas, and purification of mAbs were as described (3). All procedures were reviewed and approved by the Institute Animal Care and Use Committee.

Polyclonal Anti-ILT Serum Binding ELISA. The coh-ILT2 or Fc-ILT4 proteins were used to coat a NUNC ELISA plate at a concentration of 1 μg/mL in carbonate buffer (pH 9.6). Plates were incubated overnight at 4 °C, washed with PBS/0.05% Tween 20 (3×), and a serial dilution (in Pierce TBS blocking buffer) of the sera bleeds from the mice immunized with ILT2-Fc, ILT4-Fc, or hIgGFc alone was added to plates. Plates were incubated for 2 h at 37 °C and washed, and Pierce goat-anti-mouse IgG (H+L) (min × BvHnHs Sr prot) peroxidase conjugate was added to wells. Plates were incubated at 37 °C for 2 h, washed and analyzed following addition of TMB substrate (Zymed).

Immunofluorescent Staining of ILT on Human Skin. Human abdominal skin was obtained from healthy donors who underwent cosmetic surgeries at Baylor University Medical Center, or at Barnes Jewish Hospital in accordance with Baylor Research Institute or Washington University Institutional Review Board guidelines. Cryosections were fixed in cold acetone, dried, and blocked for nonspecific fluorescence with Fc Receptor Block and Background Buster (Innovex) and goat serum. Sections were incubated in mouse anti-CD14 (clone M5E2; 10 μg/mL) and rat anti-ILT4 (clone; 10 μg/mL) or isotype antibodies. After washing, sections were stained with goat anti-mouse AF568 (Invitrogen) and goat anti-rat AF488 (Invitrogen) and then subsequently stained with DAPI (Molecular Probes). Single channel images were acquired by using the same exposures for antibody and isotype staining, and identical scaling was applied. Single channels were then assigned color and overlaid. The digital images were taken by using an Olympus BX51 with a Planapo20×/0.7 or Planapo40×/0.95 objective, a Roper Coolsnap HQ camera, and Metamorph software (Version 6.2r6; Molecular Devices).

Structure Analysis. Combinatorial extension (4) was used to align the MHCI α1/α2 platform (aa 1–180) of the LIR-2/HLA-G [Protein Data Bank (PDB) ID code 2DYP] (5) and CD8αα/HLA-

A*0201 (PDB ID code 1AKJ) (6) crystal structures. Receptor/MHCI interfaces were analyzed by using LIGPLOT (7). PyMOL (PyMOL Molecular Graphics System; Schrödinger) was used to prepare all structure figures.

1. Bodinier M, et al. (2000) Efficient detection and immunomagnetic sorting of specific T cells using multimers of MHC class I and peptide with reduced CD8 binding. *Nat Med* 6(6):707–710.
2. Li D, et al. (2012) Targeting self- and foreign antigens to dendritic cells via DC-ASGPR generates IL-10-producing suppressive CD4+ T cells. *J Exp Med* 209(1):109–121.
3. Klechevsky E, et al. (2010) Cross-priming CD8+ T cells by targeting antigens to human dendritic cells through DCIR. *Blood* 116(10):1685–1697.
4. Shindyalov IN, Bourne PE (1998) Protein structure alignment by incremental combinatorial extension (CE) of the optimal path. *Protein Eng* 11(9):739–747.
5. Shiroishi M, et al. (2006) Structural basis for recognition of the nonclassical MHC molecule HLA-G by the leukocyte Ig-like receptor B2 (LILRB2/LIR2/ILT4/CD85d). *Proc Natl Acad Sci USA* 103(44):16412–16417.
6. Gao GF, et al. (1997) Crystal structure of the complex between human CD8alpha(alpha) and HLA-A2. *Nature* 387(6633):630–634.
7. Wallace AC, Laskowski RA, Thornton JM (1995) LIGPLOT: A program to generate schematic diagrams of protein-ligand interactions. *Protein Eng* 8(2):127–134.

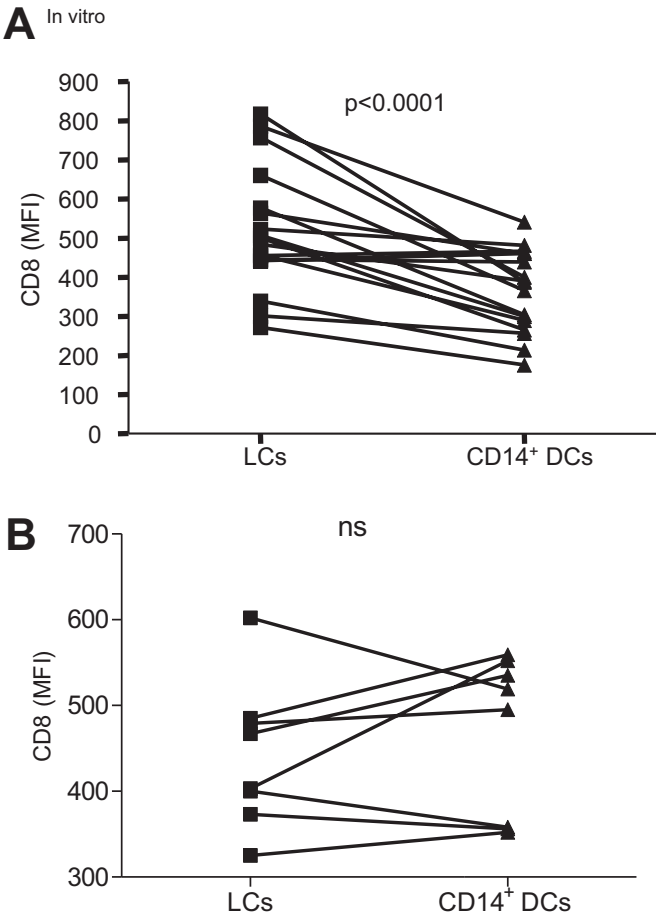

Fig. S1. Surface CD8 expression on antigen-specific T cells expanded by in vitro LCs and CD14$^+$ DCs. (*A*) CD8 mean fluorescence intensity (MFI) expression of HLA-A201–MART-1 tetramer-binding CD8$^+$ T cells, primed by in vitro CD40L-activated peptide-loaded autologous LCs and CD14$^+$ DCs. Graph shows data of 17 independent experiments. (*B*) MFI of CD8 expression by Flu-MP–specific CD8$^+$ T cells primed by autologous in vitro-generated peptide-loaded mDC subsets: LCs and CD14$^+$ DCs. Graph shows data of eight independent experiments. Results were analyzed by the paired Student *t* test.

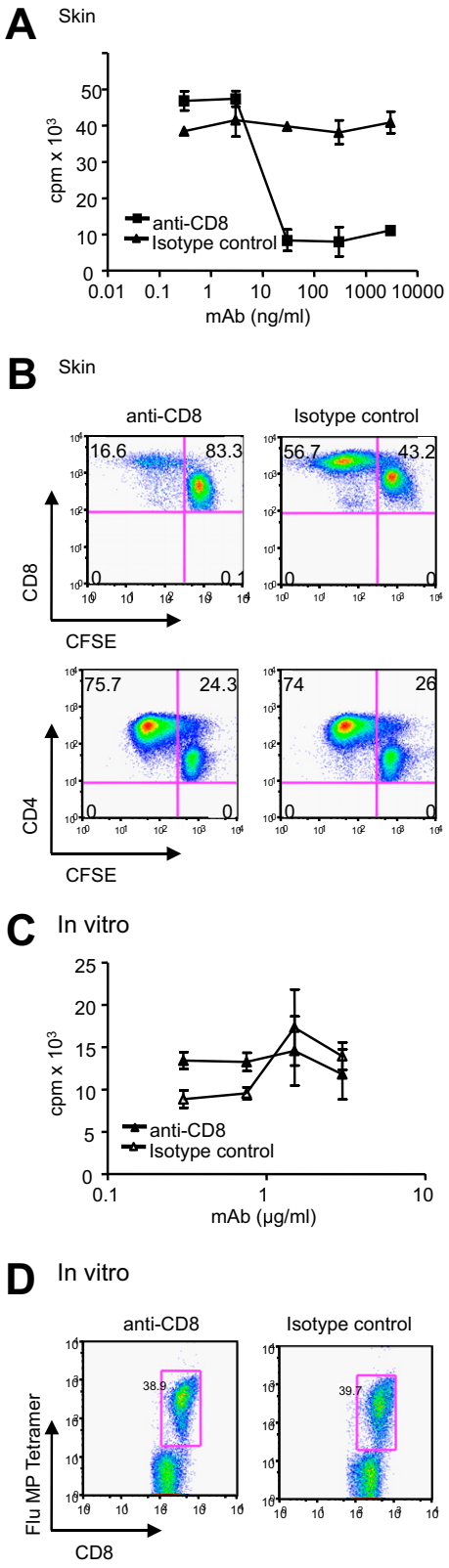

Fig. S2. Anti-CD8 mAb inhibits primary but not secondary CD8$^+$ T-cell response. (*A*) Naïve CD8$^+$ T-cell proliferation, as determined by cellular [^{3}H]thymidine incorporation, in response to allogeneic CD40L-activated skin LCs cultured for 5 d with indicated concentrations of anti-CD8 or an isotype-matched control. (*B*) Anti-CD8 mAb inhibits CD8$^+$ T cells priming against allogeneic or autologous antigens. Plots show CFSE dilution of naïve CD8$^+$ T cell (*Upper*) and CD4$^+$ T cell (*Lower*) after 7-d culture with allogeneic in vitro CD40L-activated LCs and with 1 μg/mL anti-CD8 mAb or an isotype-matched control. Memory CD8$^+$ T-cell responses are CD8-independent. (*C*) Naïve CD8$^+$ T cells were cultured with allogeneic in vitro LCs for 6 d in the presence of anti-CD8 mAb or isotype-matched control. Graph shows thymidine incorporation of CD8$^+$ T cell 3 d after a second consecutive stimulation with autologous in vitro LCs. (*D*) Flow cytometry analysis of Flu-MP-specific HLA-A201–tetramer binding CD8$^+$ T-cell expansion induced by peptide-loaded autologous in vitro LCs after 9 d of culture in the presence of 3 μg/mL anti-CD8 (RPA-T8; BD Biosciences) or an isotype-matched control. Data are representative of at least five different experiments.

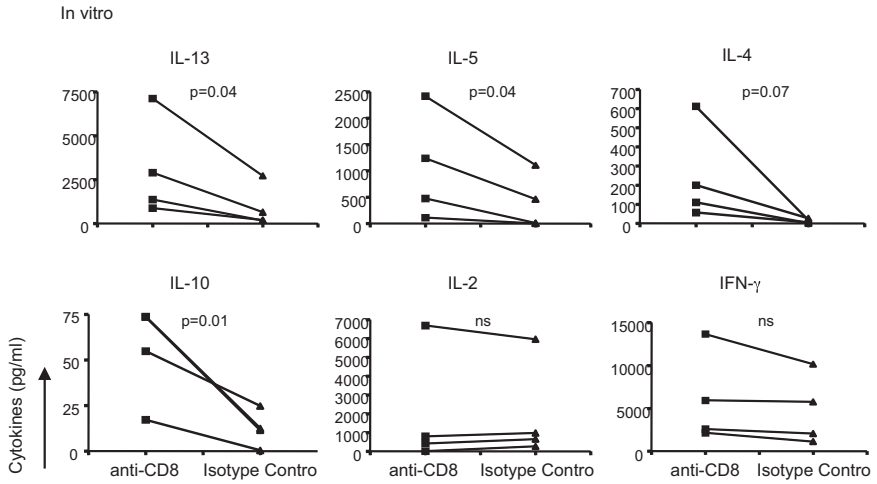

Fig. S3. Blocking CD8 leads to the generation of TC2 cells. CFSE-labeled naïve $CD8^+$ T cells were primed with allogeneic in vitro CD40L-activated LCs for 7 d. The $CFSE^{lo}$ $CD8^+$ T cells were sorted and restimulated for 24 h with anti-CD3 and -CD28 mAbs. The production of IL-13, -5, -4, -10, -2, and IFN-γ was measured in the culture supernatant by using Luminex. Graphs show data of four independent experiments.

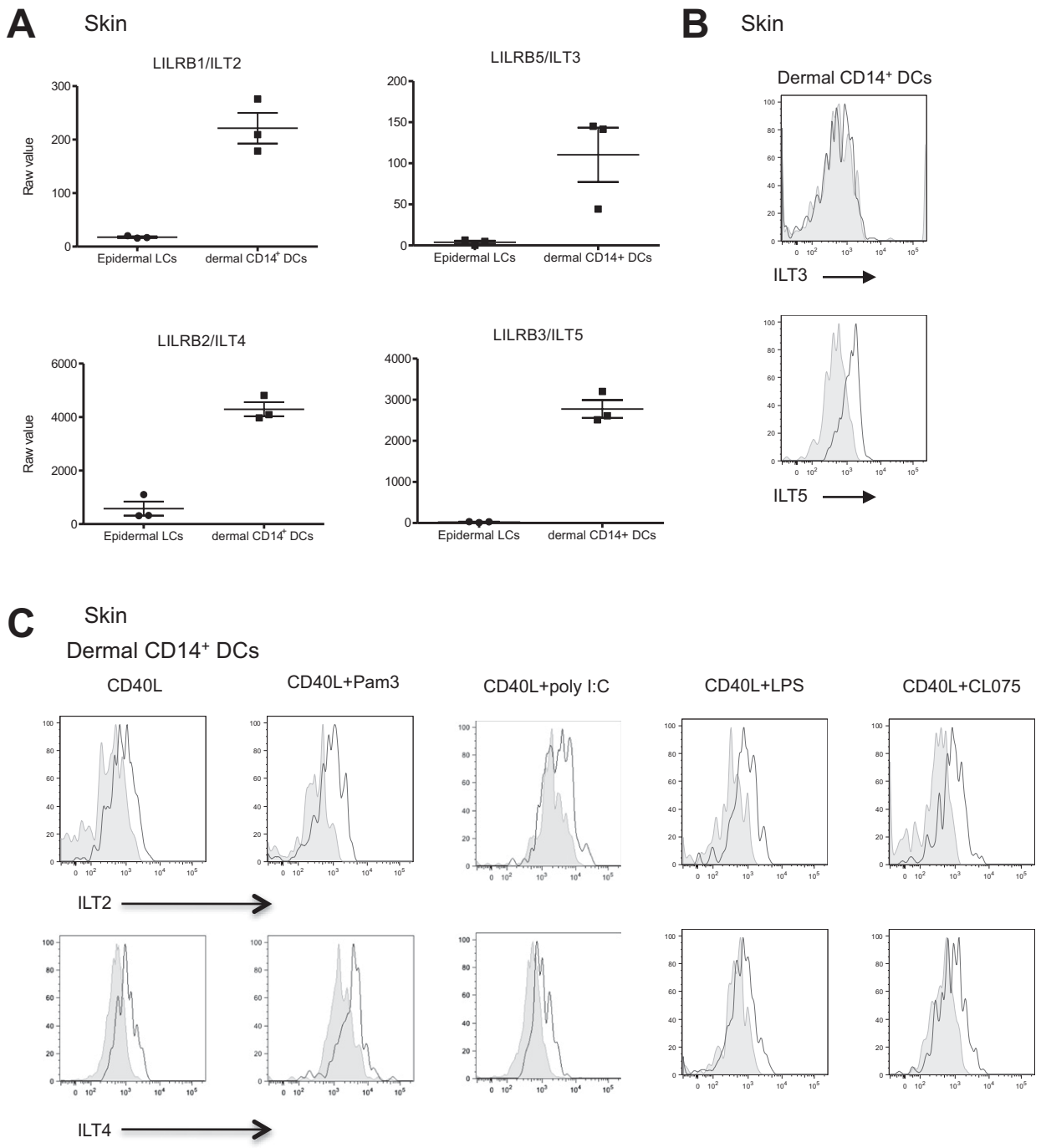

Fig. S4. Expression analysis of the ILT family receptors by the skin DC subsets. (*A*) Gene expression analysis of the ILT family receptors ILT2, ILT3, ILT4, and ILT5 by sorted skin DC subsets: LCs and dermal CD14$^+$ DCs. Graphs show that raw value gene expression of three different individuals. (*B*) Flow cytometry analysis of the ILT3 and ILT5 on the surface of skin dermal CD14$^+$ DCs (black histogram). Gray histograms represent isotype control. (*C*) The effect of TLR-agonist on ILT receptor expression by dermal CD14$^+$ DCs. Flow cytometry analysis of ILT2 and ILT4 on the surface of dermal CD14$^+$ DCs that were activated for 24 h with CD40L or a combination of CD40L and a TLR agonists: TLR2-ligand (Pam3; 50 ng/mL), TLR3-ligand (PolyI:C; 10 μg/mL), TLR4-ligand (LPS; 50 ng/mL), and TLR7/8 (CL075; 1 μg/mL). Gray curve shows cells stained with isotype-matched control mAb. Data are representative of three independent experiments.

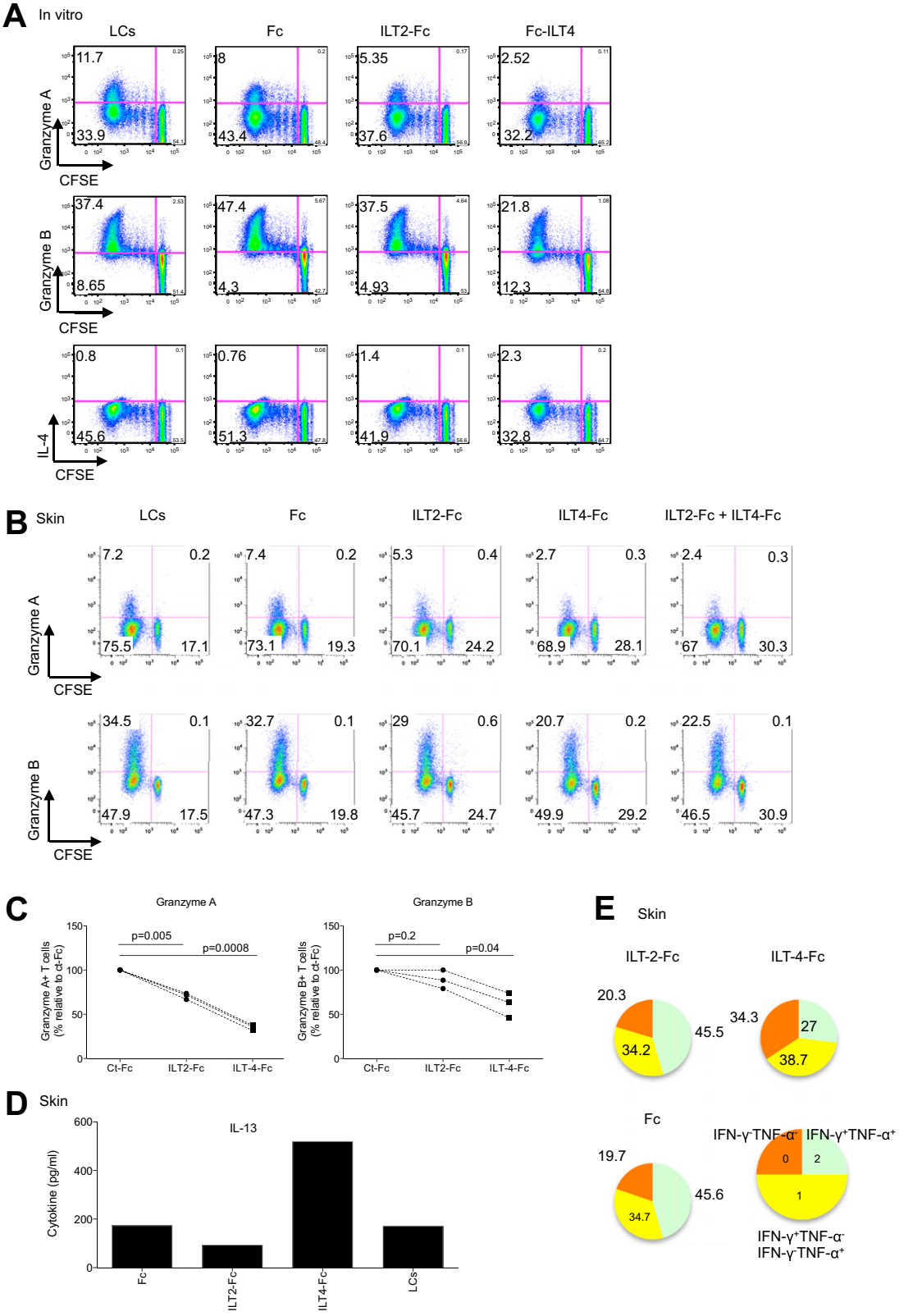

Fig. S5. Soluble ILT2 and ILT4 inhibit the generation of effector CD8$^+$ T cells by LCs. (*A*) CD40L-activated in vitro LCs were cultured at ratio of 1:20 with allogeneic CFSE-labeled naïve CD8$^+$ T cells and with the indicated Fc-fusion proteins (at 20 μg/mL). The cultures were supplemented with IL-7 and -2 on days 0 and 2, respectively. After two consecutive stimulations, the CD8$^+$ T cells were analyzed by flow cytometry for the dilution of CFSE and the intracellular expression of granzymes A and B and IL-4. (*B*) Similar to *A* using CD40L-activated skin LCs. Cells were resimulated after 9 d of culture with autologous DCs for 24 h, and the CD8$^+$ T cells were assessed by flow cytometry for the dilution of CFSE dye and the intracellular expression of granzymes A and B. (*C*) Graph shows percentage of CD8$^+$ T cells primed by LCs and ILT fusion proteins that express granzyme A (*Left*) or B (*Right*). Data of three independent experiments are shown. (*D*) Similar to

Legend continued on following page

A, after 11 d of primary culture, the $CFSE^{lo}CD11c^{-}CD4^{-}$ cells were sorted, cultured at 1.5×10^5 cells per mL, and stimulated with anti-CD3 and -CD28 mAbs for 48 h. IL-13 secretion was measured in the culture supernatant by using Luminex. (*E*) Similar to *A*, after 10 d the cells were expanded with a combination of plate bound anti-CD3, a soluble anti-CD28 mAbs and IL-2 for 24 h. The dilution of CFSE dye and intracellular expression of IFN-γ and TNF-α were assessed after additional 5-h stimulation with PMA and ionomycin with monensin. Graphs show the relative $CFSE^{lo}$ populations based on their cytokine expression profile.

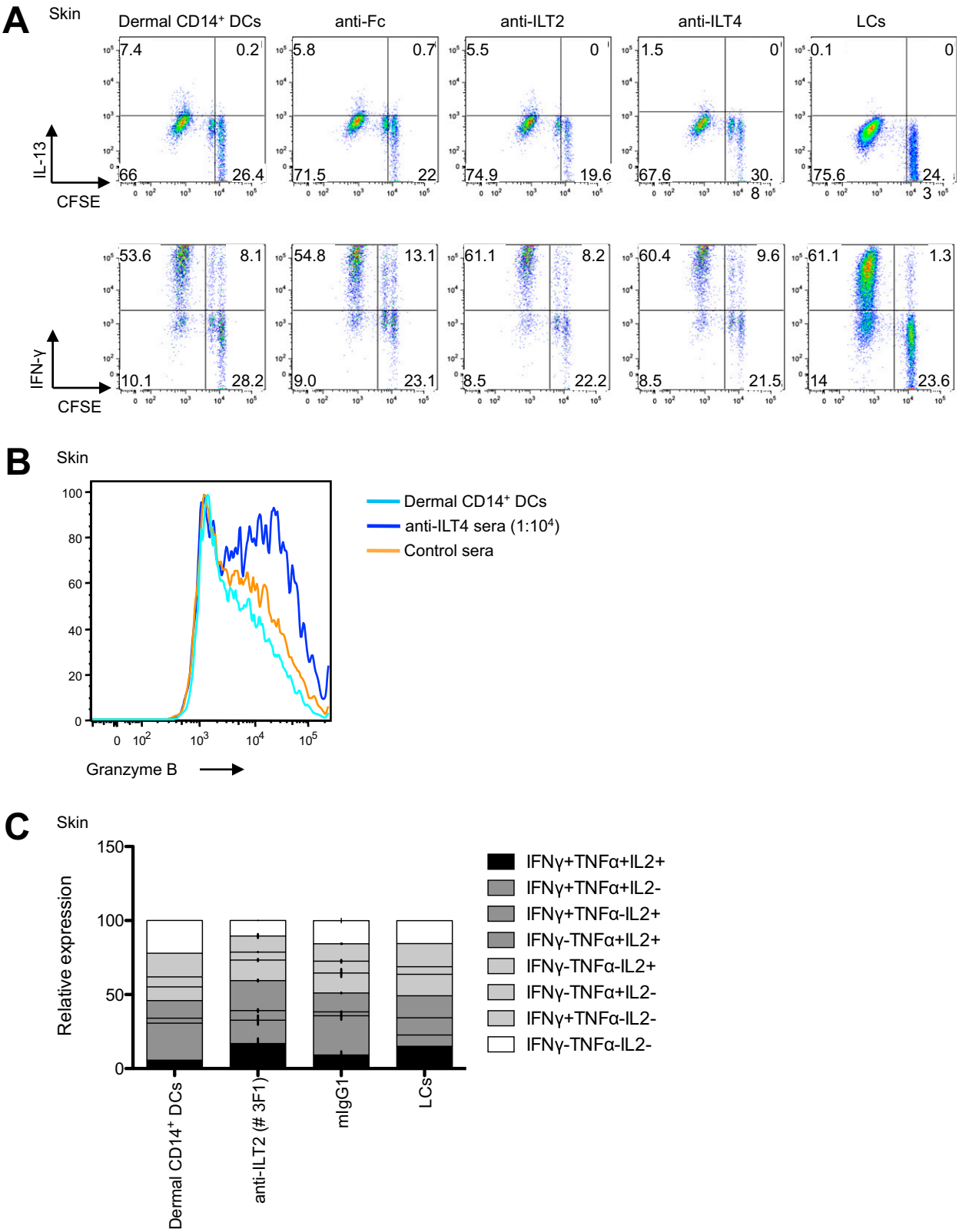

Fig. S6. Anti-ILT enhances the generation of polyfunctional CD8$^+$ T cells. (*A*) Dermal CD14$^+$ DCs were cultured at ratio 1:40 with allogeneic CFSE-labeled naïve CD8$^+$ T cells and with 1:100-dilution of serum from mice vaccinated with soluble ILT-Fc molecules. After 9 d, the cells were expanded with anti-CD3 and -CD28 mAbs and IL-2 for 48 h and assessed following 5 h of reactivation with PMA and ionomycin for the dilution of CFSE dye and intracellular expression of IL-13 and IFN-γ by flow cytometry. CD8$^+$ T cells cultured with skin LCs served as a control. (*B*) Dermal CD14$^+$ DCs were cultured at a ratio of 1:40 with allogeneic CFSE-labeled naïve CD8$^+$ T cells and 1:100-dilution of pooled serum from three mice vaccinated with a soluble ILT4-Fc or a control Fc fusion proteins. After 9 d the cells were assessed by flow cytometry for the expression of intracellular granzyme B. Histogram shows the relative expression by the cells that diluted CFSE dye.

Legend continued on following page

(*C*) mAbs specific to anti-ILT2 (mouse IgG1 clone 3F1) were added at 20 μg/mL to cocultures of dermal CD14$^+$ DCs and naïve CD8$^+$ T cells. As in *A*, the cells were analyzed by flow cytometry for the expression of intracellular IFN-γ, TNF-α, and IL-2. CD8$^+$ T cells cultured with skin LCs served as a control. Graph shows the relative populations based on their cytokine expression profile.

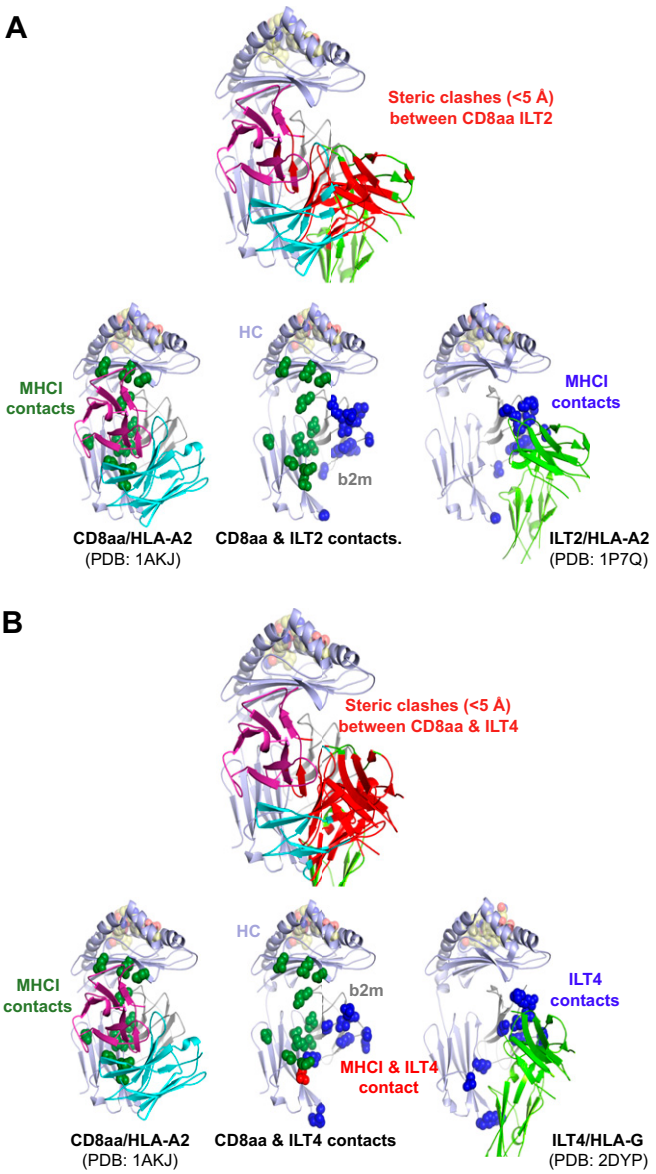

Fig. S7. CD8αα and ILT2 or ILT4 exclude each other sterically. (*A*) ILT2 and CD8αα cannot simultaneously engage MHC class I. The MHC class I α1/α2 platform of the ILT2/HLA-A2 (PDB ID code 1P7Q) (3) and CD8αα/HLA-A-0201 (PDB ID code 1AKJ) (2) crystal structures were aligned to examine the potential steric/contact overlap between ILT2 and CD8αα. Complexes are shown as ribbon diagrams: CD8αα (cyan/magenta), ILT2 (light green), heavy chain (blue), β2m (gray), peptide (yellow, spheres). (*Upper*) Ribbon diagram of significant steric clashes (≤5 Å, red) between ILT2 and CD8αα that would occur if both receptors engaged MHCI. (*Lower*) Contacts for each receptor/MHCI complex are shown as spheres: CD8αα (dark green), ILT2 (blue). Receptors were omitted in (*Lower Center*) for clarity. LIGPLOT analysis did not identify contacts shared by CD8αα and ILT2. (*B*) ILT4 and CD8-αα cannot simultaneously engage MHC class I: The MHCI α1/α2 platform of the ILT4/HLA-G (PDB ID code 2DYP) (1) and CD8αα/HLA-A*0201 (PDB ID code 1AKJ) (2) crystal structures were aligned to examine the potential steric/contact overlap between ILT4 and CD8αα. Complexes are shown as ribbon diagrams: CD8αα (cyan/magenta), ILT4 (light green), heavy chain (blue), β2m (gray), peptide (yellow, spheres). (*Upper*) Ribbon diagram of significant steric clashes (≤5 Å, red) between ILT4 and CD8αα that would occur if both receptors engaged MHCI. HLA-G was omitted from this figure. (*Lower*) Contacts for each receptor/MHCI complex are shown as spheres: CD8αα (dark green), ILT4 (blue), CD8αα and ILT4 (red, D227). Receptors were omitted in *Lower Center* for clarity.

1. Shiroishi M, et al. (2006) Structural basis for recognition of the nonclassical MHC molecule HLA-G by the leukocyte Ig-like receptor B2 (LILRB2/LIR2/ILT4/CD85d). *Proc Natl Acad Sci USA* 103(44):16412–16417.
2. Gao GF, et al. (1997) Crystal structure of the complex between human CD8alpha(alpha) and HLA-A2. *Nature* 387(6633):630–634.
3. Willcox BE, Thomas LM, Bjorkman PJ (2003) Crystal structure of HLA-A2 bound to LIR-1, a host and viral major histocompatibility complex receptor. *Nat Immunol* 4(9):913–919.